0022-3565/10/3342-364–372$20.00
THE JOURNAL OF PHARMACOLOGY AND EXPERIMENTAL THERAPEUTICS
JPET 334:364–372, 2010

Vol. 334, No. 2
165001/3603503
Printed in U.S.A.

PRX-08066, a Novel 5-Hydroxytryptamine Receptor 2B Antagonist, Reduces Monocrotaline-Induced Pulmonary Arterial Hypertension and Right Ventricular Hypertrophy in Rats

Stacy L. Porvasnik, Sean Germain, Jennifer Embury, Kimberley S. Gannon, Vincent Jacques, Justin Murray, Barry J. Byrne, Sharon Shacham, and Faris Al-Mousily

Department of Pediatrics (S.L.P., S.G., B.J.B., F.A.), Powell Gene Therapy Center (S.L.P., S.G., B.J.B.), and Departments of Biochemistry and Molecular Biology (J.E.) and Animal Care Services (J.M.), University of Florida, Gainesville, Florida; EPIX Pharmaceuticals, Lexington, Massachusetts (V.J., S.S.); and Eolas Biosciences USA, Watertown, Massachusetts (K.S.G.)

Received January 5, 2010; accepted April 28, 2010

ABSTRACT

Pulmonary arterial hypertension (PAH) is a life-threatening disease that results in right ventricular failure. 5-((4-(6-Chlorothieno[2,3-d]pyrimidin-4-ylamino)piperidin-1-yl)methyl)-2-fluorobenzonitrile monofumarate (PRX-08066) is a selective 5-hydroxytryptamine receptor 2B (5-HT2BR) antagonist that causes selective vasodilation of pulmonary arteries. In the current study, the effects of PRX-08066 were assessed by using the monocrotaline (MCT)-induced PAH rat model. Male rats received 40 mg/kg MCT or phosphate-buffered saline and were treated orally twice a day with vehicle or 50 or 100 mg/kg PRX-08066 for 5 weeks. Pulmonary and cardiac functions were evaluated by hemodynamics, heart weight, magnetic resonance imaging (MRI), pulmonary artery (PA) morphology, and histology. Cardiac MRI demonstrated that PRX-08066 (100 mg/kg) significantly ($P < 0.05$) improved right ventricular ejection fraction. PRX-08066 significantly reduced peak PA pressure at 50 and 100 mg/kg ($P < 0.05$ and < 0.01, respectively) compared with MCT control animals. PRX-08066 therapy also significantly reduced right ventricle (RV)/body weight and RV/left ventricle + septum ($P < 0.01$ and < 0.001, respectively) compared with MCT-treated animals. Morphometric assessment of pulmonary arterioles revealed a significant reduction in medial wall thickening and lumen occlusion associated with both doses of PRX-08066 ($P < 0.01$). The 5-HT2BR antagonist PRX-08066 significantly attenuated the elevation in PA pressure and RV hypertrophy and maintained cardiac function. Pulmonary vascular remodeling was also diminished compared with MCT control rats. PRX-08066 prevents the severity of PAH in the MCT rat model.

Pulmonary arterial hypertension (PAH) is an elevation in pulmonary vascular resistance caused by vasoconstriction and pulmonary vascular remodeling, resulting in increased pulmonary arterial pressure. Idiopathic PAH has no known underlying cause. PAH can also develop as a consequence of coexisting disease, such as chronic obstructive pulmonary disease, hypoxia, portal hypertension, or HIV infection (Archer and Rich, 2000; Li et al., 2006). PAH is usually progressive and invariably fatal. The median survival without treatment in adult patients with PAH was 2.8 years after diagnosis, and in children the median survival was only 10 months (D'Alonzo et al., 1991). Recent advances in PAH therapies, specifically epoprostenol-treated patients, have resulted in the median survival reaching more than 6 years in adults (Barst et al., 1994) and significant improvement in survival for children with reported rates at 1, 5, and 10 years being 94, 81, and 61%, respectively (Yung et al., 2004). Although survival rates have improved with new therapeutic modalities, the prognosis is still poor and development of more effective therapies is clearly needed.

Serotonin or 5-hydroxytryptamine (5-HT) was recognized for playing a role in the development of PAH because a relationship between PAH patients and diet pills such as aminorex, dexfenfluramine (DF), and fenfluramine was observed (Kew, 1970;

This research was funded by EPIX Pharmaceuticals, the developer of PRX-08066.
Article, publication date, and citation information can be found at http://jpet.aspetjournals.org.
doi:10.1124/jpet.109.165001.

ABBREVIATIONS: PAH, pulmonary arterial hypertension; PRX-08066, 5-((4-(6-chlorothieno[2,3-d]pyrimidin-4-ylamino)piperidin-1-yl)methyl)-2-fluorobenzonitrile monofumarate; PH, pulmonary hypertension; 5-HT, 5-hydroxytryptamine; 5-HT2BR, 5-HT receptor 2B; AE, alveolar edema; AMI, alveolar macrophage infiltration; DF, dexfenfluramine; LV, left ventricle; LV+S, LV + septum; MCT, monocrotaline; OLP, overall lung pathology; PA, pulmonary artery; PAP, peak pulmonary artery pressures; PBS, phosphate-buffered saline; PE, perivascular edema; RV, right ventricle; ANOVA, analysis of variance; H&E, hematoxylin-eosin; VH, vehicle; MR, magnetic resonance; MRI, MR imaging; NS-304, 2-{4-[(5,6-diphenylpyrazin-2-yl)(isopropyl)amino]butoxy}-*N*-(methylsulfonyl)acetamide; RS-127445, 4-(4-fluoro-1-naphthyl)-6-isopropylpyrimidin-2-amine; PVR, pulmonary vascular resistance.

Kay et al., 1971; Kramer and Lane, 1998). 5-HT remodels the pulmonary vasculature associated with PAH by vasoconstriction, promotion of platelet aggregation, and pulmonary arterial smooth muscle cell proliferation (Egermayer et al., 1999; MacLean et al., 2000; Dempsie and MacLean, 2008). Of the 14 different 5-HT receptors, the 5-HT1B, 5-HT2A, and 5-HT2B receptors show evidence in playing a role in the pathobiology of PAH (MacLean, 2007). 5-HT2B receptors (5-HT2BRs) are expressed in pulmonary endothelial and smooth muscle cells and stimulate calcium release in human endothelial cells from the pulmonary artery (Esteve et al., 2007). In the chronic hypoxic mouse model of pulmonary hypertension (PH), researchers demonstrated that 5-HT2BRs are involved in the development of PH by mediating chronic hypoxic responses in wild-type mice compared with the complete absence of PH and vascular remodeling in 5-HT2BR(−/−) mice (Launay et al., 2002). Both aminorex and fenfluramine cause an elevation of 5-HT levels by increasing the release of 5-HT from platelets and inhibiting the metabolisms or the reuptake of 5-HT (MacLean, 1999; Fitzgerald et al., 2000; Belohlávková et al., 2001). Whereas DF binds weakly to the 5-HT2A, 5-HT2B, and 5-HT2C receptors, its main metabolite, *N*-deethylated DF is a potent agonist of the 5-HT2BR (Hong et al., 2004). These results suggest that 5-HT2BR may play a critical role in the development of PAH pathogenesis.

5-((4-(6-Chlorothieno[2,3-d]pyrimidin-4-ylamino)piperidin-1-yl)methyl)-2-fluorobenzonitrile monofumarate (PRX-08066) (Orbach et al., 2006) is a highly potent (K_i ~3.4 nM) and selective 5-HT2BR antagonist that causes selective vasodilation of pulmonary arteries (Orbach et al., 2006). In a series of in vitro studies designed to test the effect of PRX-08066 on 5-HT-induced vascular muscularization, PRX-08066 inhibited 5-HT-induced mitogen-activated protein kinase activation (IC_{50} ~12 nM) and markedly reduced thymidine incorporation (IC_{50} ~3 nM) in Chinese hamster ovary cells expressing the human 5-HT2BR. This suggests that PRX-08066 can potentially inhibit the pathologic 5-HT-induced vascular muscularization associated with PAH. PRX-08066 significantly reduced the hypoxia-dependent increase in right ventricular systolic pressure in both rats and mice without affecting the systemic mean arterial pressure in the animals (Orbach et al., 2006). PRX-08066 has the potential to provide direct and selective vasodilation of the pulmonary vasculature without affecting systemic blood pressure.

We selected the monocrotaline (MCT)-induced rat model of PH because it is well documented that 5-HT plays an important role in the pathogenesis of MCT-induced PH (Kanai et al., 1993; Miyata et al., 2000). MCT-induced PH in rats is a commonly used animal model of inflammatory PH that produces endothelial injury and changes to the pulmonary vasculature similar to human forms of PAH. In this study, we investigated the effect of PRX-08066 to determine whether this 5-HT2BR antagonist could prevent or reduce the severity of MCT-induced PH.

Materials and Methods

Formulation of PRX-08066. A suspension of PRX-08066 at 20 mg/ml for oral gavage was developed. The compound was weighed and suspended in water, and the pH was adjusted to between 6.5 and 7.5 by the slow addition of 1 N NaOH (sodium hydroxide). Methylcellulose in water (1% w/v) and 10× phosphate-buffered saline (PBS) were added to achieve a final concentration of 20 mg/ml PRX-08066 in 0.5% methylcellulose (w/v) and 1× PBS. The suspension was wrapped in aluminum foil and stored at room temperature. The suspension was kept homogeneous by continuous stirring before dosing.

MCT-Induced PAH in Rats and Experimental Design. Male Sprague-Dawley rats (Harlan, Indianapolis, IN) weighing between 200 and 225 g were housed in conventional conditions in the Animal Care Services Facility at the University of Florida. All experiments were approved by the Institutional Animal Care and Use Committee at the University of Florida. Before entering the study, rat hearts were prescreened for any abnormalities by echocardiography using a Phillips Sonos 5500 echo machine (Hewlett Packard, Palo Alto, CA) with a 12-MHz ultrasound probe.

The rats were randomly assigned to four experimental groups: 1) PBS control + vehicle (VH) (n = 10); 2) MCT + vehicle (n = 10); 3) MCT + 50 mg/kg PRX-08066 (n = 8); and 4) MCT + 100 mg/kg PRX-08066 (n = 13). Compound PRX-08066 or VH, 0.5% methylcellulose (w/v), and 1× PBS were administered twice daily by oral gavage for 5 weeks. PAH was induced on day 0 approximately 2 to 4 h after the first gavage treatment by a single dose of MCT (40 mg/kg s.c.) (Sigma-Aldrich, St. Louis, MO). Rats were weighed twice a week, and dosages were adjusted appropriately. At the end of the 4-week treatment regimen each rat was assessed for PAH by using cardiac magnetic resonance imaging (MRI). At the end of 5 weeks, invasive hemodynamic measurements were assessed, blood samples were taken, and the rats were sacrificed.

Quantitation of PRX-08066 in Blood Plasma. Blood samples were collected in potassium EDTA tubes 2 h after morning dose on days 4, 7, 14, and 21 and centrifuged at 5500*g* for 10 min. Plasma samples were mixed with three volumes of acetonitrile containing reserpine (Sigma-Aldrich) as an internal standard. Precipitate and supernatant were separated by centrifugation, and the supernatant was analyzed by liquid chromatography/mass spectrometry using the Agilent 1100 HPLC system (Agilent Technologies, Santa Clara, CA), equipped with a Waters Symmetry C18 column, 2.1 × 30 mm (Waters, Milford, MA); solvent A, 0.1% formic acid in water and solvent B, 0.1% formic acid in acetonitrile; 1.5 ml/min gradient elution from 90% to 50% of solvent A in 2 min to 5% in 0.5 min to 90% in 0.3 min; total run time 3.5 min; LC/MSD Trap XCT Ultra (Thermo Fisher Scientific, Waltham, MA) in electrospray positive ion mode using transitions m/z 403.2 → 217.1 for PRX-08066 and 609.7 → 448.0 for reserpine.

PRX-08066 concentration was determined by interpolation with a standard curve obtained from $1/x^2$-weighted linear regression of peak-to-internal standard ratios of calibration standards to their respective nominal concentration. Standards were prepared by spiking PRX-08066 in blank plasma using the protocol described above for unknown samples.

Magnetic Resonance Imaging. MRI of the rat cardiac cycle was performed with a 4.7-Tesla Bruker Avance spectrometer (Bruker Biospin, Billerica, MA). The rats were anesthetized by using a mixture of 1.5 to 2% isoflurane and oxygen (O_2). Monitoring of respiration and electrocardiogram for use during data acquisition was conducted by using a small animal instrument monitoring and gating system (S/A Instruments, Inc., Stony Brook, NY). Rats were placed in the prone position on a quadrature surface receive/quadrature volume transmit coil and inserted feet first into the magnet. After the acquisition of an ungated survey sequence, two- and four-chamber cine sequences were acquired by using a fast low-angle shot sequence (repetition time, ~200 ms; echo time, 2.5 ms; matrix, 256 × 128; field of view, 70 × 30 mm; thickness, 1 mm; three slices) to prescribe short axis images. After identification of the most apical and basal segments of the ventricles using the two- and four-chamber images, a short axis image stack was collected with a fast low-angle shot sequence (repetition time, ~200 ms; echo time, 2.7 ms; matrix, 256 × 192; field of view, 40 × 30 mm; thickness, 1 mm; approximately 12 slices). The rat's electrocardiogram was used to trigger each phase encode segment at the peak of the R wave. Repetition time depended on the heart rate of the animal and R-R

interval. Approximately 14 to 20 frames were used to capture the entire cardiac cycle. Right ventricle (RV) and left ventricle (LV) volumetric and RV wall thicknesses (in short axis midventricle images) measurements were performed by using CAAS MRV FARM software (Pie Medical Imaging, Maastricht, The Netherlands).

Invasive Hemodynamic Analysis. To obtain peak pulmonary artery pressures (PAP), the rats were anesthetized with isoflurane at 4 to 5% in 100% O_2 then intubated intratracheally with a 14-gauge angiocatheter and placed on an SAR-830 small animal ventilator (CWE, Inc., Ardmore, PA). The isoflurane was decreased to a flow rate of 2.0% with an O_2 flow rate of 0.3 L/min maintained at 1.7 ml of tidal volume and respiratory rate of 65 breath/min. The rat's chest was opened to expose the heart. A 1.4F Millar MIKRO-TIP catheter transducer (Millar Instruments Inc., Houston, TX) was inserted directly into the left ventricle to record left ventricular pressure. After the left ventricular pressure was recorded, the Millar catheter was removed, inserted into the right ventricle and advanced into the PA to record right ventricular pressure and PAP. The hemodynamic tracings were evaluated by using Power Lab equipment and software (Power Lab version 5.2.2; ADI Instruments, Castle Hill, Australia).

RV Hypertrophy and Histology Samples. The rats were perfused with PBS through the left ventricle over 5 min with a 24-g angiocatheter after blood samples were collected. The hearts were removed and weighed. The great arteries and atria were removed, and the ventricles were dissected apart. The free right ventricle wall and the left ventricle with septum were weighed. The left lung and liver were excised and divided into 2-mm-thick sections. The tissues were fixed in 10% neutral buffered formalin for 8 h, transferred to 70% ethyl alcohol, and embedded in paraffin. Four-micrometer tissue sections were cut and stained with hematoxylin-eosin (H&E). An extra lung slide was cut and stained by the Verhoeff-van Gieson method to highlight the elastic lamina of the pulmonary arteries.

Evaluation of Histopathology. Histological evaluation was completed on 41 lung H&E slides. Tissues were scored by a pathologist blinded to the experimental conditions. The following parameters were evaluated in the lung tissue: alveolar edema (AE), alveolar macrophage infiltrate, type II pneumocyte hyperplasia, general arterial thickening, thickening of tunica intima, thickening of tunica media, and perivascular edema (PE). Each parameter was evaluated and scored from 0 to 5, with 0 being no discernable lesions and 5 indicating the most severe lesions. Final scores for the overall lung pathology (OLP) were calculated by averaging all parameters for each individual treatment group. The experimental groups were revealed after the histological scoring was completed, and individual animals were placed in the appropriate groups for statistical analysis.

Morphometric Analysis of Pulmonary Arteries. Lung slides stained with Verhoeff-van Gieson were used to measure arterioles ranging from 25 to 100 μm for muscularization of medial wall thickness at a magnification of ×400. Fifteen arteriole images per lung section were taken with a Zeiss Axioskop microscope, Axiocam camera, and AxioVision software (Carl Zeiss, Inc., Thornwood, NY). MetaMorph Offline imaging software (MetaMorph Imaging System; Molecular Devices, Sunnyvale, CA) was used to calculate the area of the lumen and the area of total vessel. A ratio of lumen area to total vessel area multiplied by 100 (L/TV%) was then calculated as a relative measurement of arteriole wall thickness and lumen-carrying capacity (Ohar et al., 1998; Zhou et al., 2006).

Statistical Analysis. All data are expressed as means ± S.E.M. unless otherwise indicated. Differences between treatment groups were analyzed by using one-way ANOVA and a post-hoc Tukey multiple comparison test. Comparison between variables measured was completed by using a Pearson correlation test. $P < 0.05$ was considered statistically significant.

Results

Stability of PRX-08066 Plasma Concentrations. PRX-08066 plasma levels were measured 2 h after dose (t_{max}) every week throughout the study. Plasma levels were stable throughout the study (Fig. 1), and drug concentration increased approximately 2-fold with a 2-fold increase in dose as expected from a linear pharmacokinetic behavior. Indeed, averages of all plasma levels were 2780 ± 180 (n = 48 measurements) and 1250 ± 110 ng/ml plasma (n = 32) at doses of 100 and 50 mg/kg, respectively. Stable plasma levels of PRX-08066 at 2 h after dose confirmed that there was no accumulation of drug and no increase in elimination over the course of the study. During week 4 of dosing, plasma levels were determined at 6 to 7 h after dose (trough) and found to be 835 ± 209 and 328 ± 60 ng/ml at doses of 100 and 50 mg/kg, respectively.

Correction of Cardiac Function Determined by MRI. Diastolic and systolic images are illustrated in Fig. 2 for all four experimental groups. PRX-08066-treated groups (Fig. 2, A, B, E, and F) demonstrated less right ventricular hypertrophy and septal flattening than the MCT control group (Fig. 2, C and G). In MCT rats that were treated with 100 mg/kg PRX-08066 the RV mass was significantly decreased compared with the MCT + VH group as seen in Fig. 2I (293 mg ± 16.69 and 458 mg ± 38.10, respectively; $P < 0.001$) and approached the normal RV mass value of the PBS + VH control group (265 mg ± 10.29). The 50 mg/kg dose of PRX-08066 showed less severe RV hypertrophy but was not significant (342.4 mg ± 46.69) when analyzed with the MCT control. The RV ejection fraction (Fig. 2J) of rats treated with 50 mg/kg PRX-08066 (55.41 ± 6.12) and 100 mg/kg PRX-08066 was greater than that of the MCT + VH rats, but only the MCT + 100 mg/kg PRX-08066 group reached statistical significance at 57.44 ± 2.6 versus 41.46 ± 4.39 ($P < 0.05$). However treatment of PRX-08066 after 4 weeks increased RV ejection fractions closer to normal cardiac values demonstrated by the PBS + VH control rats (66.00 ± 1.71).

The positive effects of PRX-08066 treatment on RV remodeling resulted in preserved LV diastolic, systolic, and stroke volume (Fig. 3). The LV diastolic volumes (Fig. 3A) for the 50 mg/kg (461 μl ± 45.87) and 100 mg/kg (473.8 μl ± 20.77) groups of PRX-08066 were significantly maintained close to

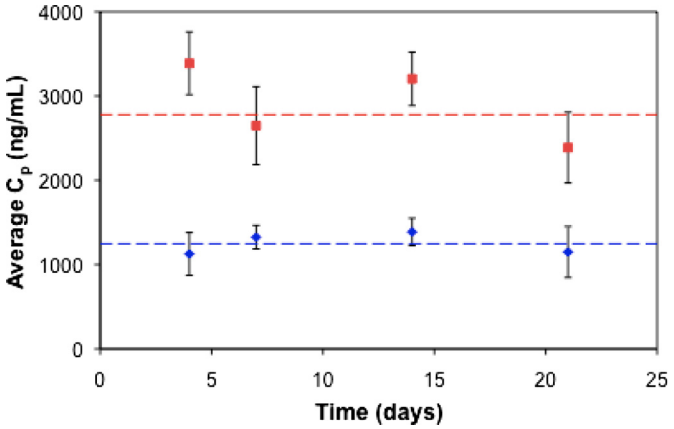

Fig. 1. Plasma levels of PRX-08066 in both dose groups shows linear pharmacokinetic behavior (red squares, 100 mg/kg; blue diamonds, 50 mg/kg; dashed lines represent mean value throughout study). Data are presented as mean ± S.E.M.

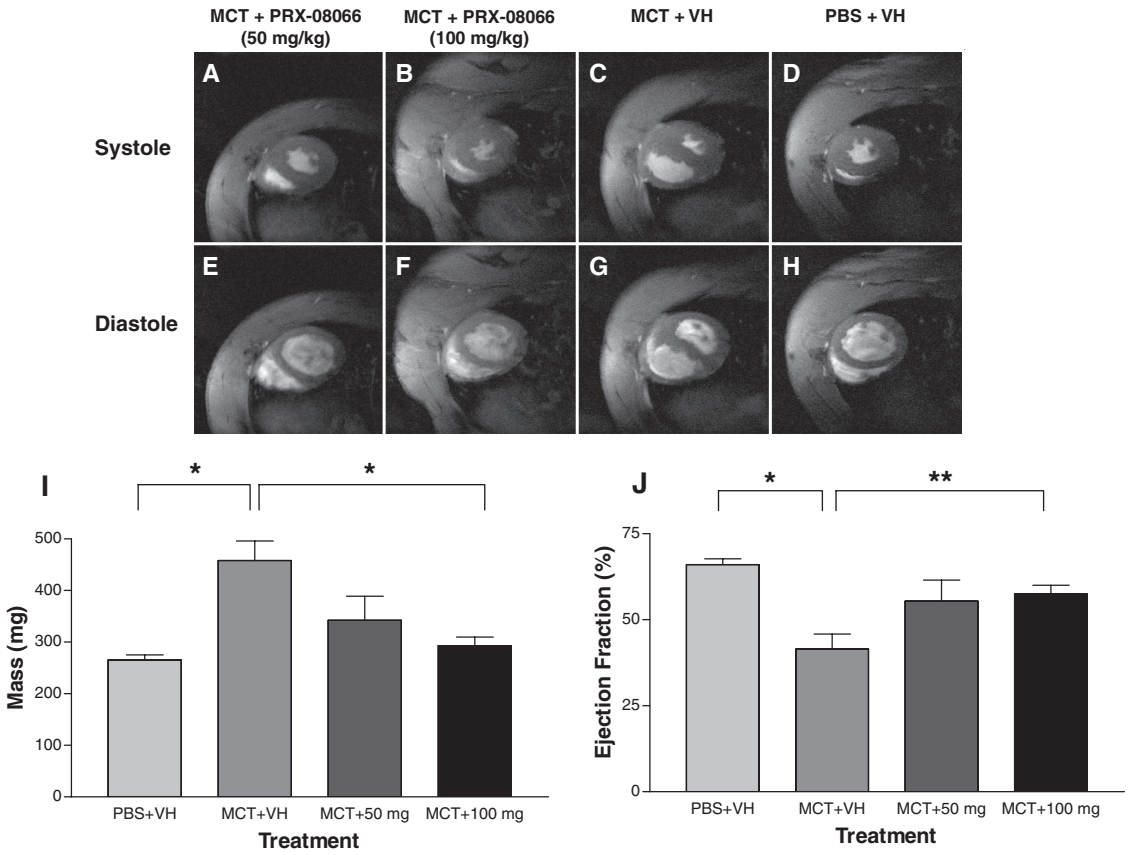

Fig. 2. MRI assessment of RV mass and ejection fraction after 4 weeks of PRX-08066 treatment. A–H, representative systolic and diastolic heart images from MCT + 50 mg/kg PRX-08066 (A and E), MCT + 100 mg/kg PRX-08066 (B and F), MCT + VH (C and G), and PBS + VH (D and H) treatment groups. I, RV mass calculated from MR images for all four experimental groups. RV mass was lower in the 100 mg/kg dose of PRX-08066 (*, $P < 0.001$), whereas the 50 mg/kg treatment group was not significantly decreased. J, MRI RV ejection fraction in PRX-08066-treated rats. Rats treated with the higher dose of PRX-08066 showed the most improvement (*, $P < 0.001$; **, $P < 0.05$). Data are shown as the mean ± S.E.M.

normal values over the MCT + VH group (287.8 μl ± 41.33; $P < 0.01$ and < 0.001, respectively). The MCT + 100 mg/kg PRX-08066 group also maintained a significantly higher LV systolic volume (Fig. 3B) compared with the MCT + VH control (164.4 μl ± 13.84 versus 112.8 μl ± 17.30; $P < 0.05$). The LV stroke volume increased significantly with treatment by PRX-08066 (Fig. 3C). The LV stroke volumes of the PBS + VH and the MCT + 100 mg/kg PRX-08066 rats (347.40 μl ± 11.47 and 309.40 μl ± 8.67, respectively) were significantly higher than in the MCT + VH rats (175.1 μl ± 25.71; $P < 0.001$). Rats receiving the MCT + 50 mg/kg PRX-08066 dose (295 μl ± 33.70) also showed beneficial effects compared with the MCT + VH rats ($P < 0.01$).

Changes in Hemodynamic Variables after Treatment of PRX-08066. The hemodynamic variables after 5 weeks of treatment with PRX-08066 were greatly improved (Fig. 4). Compared with the MCT control group (63.44 mm Hg ± 7.78), peak PAP in the groups receiving MCT + 50 mg/kg PRX-08066 and MCT + 100 mg/kg PRX-08066 (Fig. 4A) were significantly decreased (43.07 mm Hg ± 5.10, $P < 0.05$ and 40.75 mm Hg ± 3.47, $P < 0.01$, respectively). The peak PAP in the MCT + VH group was notably elevated by a 2-fold increase compared with the PBS + VH group (26.95 mm Hg ± 1.24; $P < 0.001$). No significant difference was observed in the peak LV pressure (Fig. 4B). The peak RV/LV ratio shown in Fig. 4C was significantly lower in the rats with MCT + 100 mg PRX-08066 (0.43 ± 0.04) compared with the rats with MCT + VH (0.75 ± 0.10; $P < 0.01$), indicating PRX-08066 had a favorable effect on the prevention and modulation of pathological changes initiated by the MCT injection.

Effects of PRX-08066 on Body Weight and RV Hypertrophy. Comparison and statistical analysis of body weight and ventricular remodeling from all four experimental groups can be seen in Table 1. Rats in the MCT + 50 mg/kg PRX-08066 treatment group gained significantly more weight than rats receiving MCT + VH ($P < 0.01$). The weight gain observed for rats receiving MCT + 100 mg/kg PRX-08066 was not significant compared with the MCT + VH control group.

Rats treated with 50 and 100 mg/kg PRX-08066 demonstrated a marked reduction in RV hypertrophy illustrated by the RV necropsy mass-to-body-weight ratio (Table 1). PRX-08066 attenuated RV hypertrophy after 5 weeks of treatment by 32 to 34% after MCT induction. The MCT + VH control rats developed a 2-fold increase of RV hypertrophy over the PBS + VH control rats. The RV/LV+ S ratio was also significantly decreased in the PRX-08066-treated groups compared with the MCT + VH group.

Relationship between MRI-Derived RV Performance and Invasive Outcome Measures. The positive correlation seen between the calculated MRI RV end-diastolic myocardial mass and the RV mass obtained at necropsy ($P < 0.0001$; $r = 0.82$) is shown in Fig. 5A. This signifies that the robust

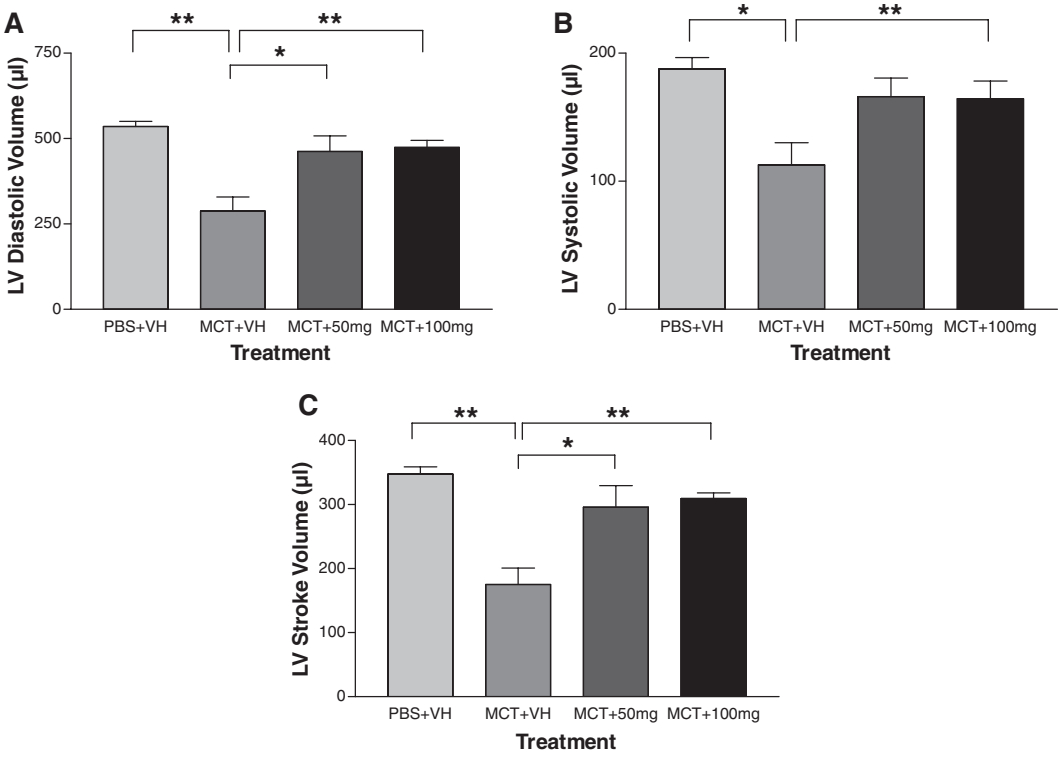

Fig. 3. LV diastolic, systolic, and stroke volumes were measured from MR images. A, the LV diastolic volume was increased in rats that received treatment from PRX-08066 (*, $P < 0.01$; **, $P < 0.001$) compared with the MCT + VH group. B, rats treated with 50 and 100 mg/kg PRX-08066 also showed marked improvement in LV systolic volume (*, $P < 0.01$; **, $P < 0.05$). C, the beneficial effects of 50 and 100 mg/kg PRX-08066 were significantly demonstrated by an increase in LV stroke volume compared with the MCT + VH group (*, $P < 0.01$; **, $P < 0.001$). Data are shown as the mean ± S.E.M.

noninvasive tool MRI can be used to follow stages of PAH. RV hypertrophy, MRI RV-derived mass, as a function of peak PAP ($P < 0.0001$; $r = 0.78$) depicts the RV overload that occurs as the pulmonary arterial vasculature thickens (Fig. 5B). A negative correlation was observed between the RV/LV+S mass ratio and the MRI RV ejection fractions ($P < 0.0001$; $r = -0.84$), illustrating how PRX-08066-treated rats have increased ejection fractions compared with the MCT + VH animals (Fig. 5C).

Histological Changes with PRX-08066 Treatment on Development of MCT-Induced PH. Treatment with 50 and 100 mg/kg PRX-08066 reduced the following pathological features associated with MCT-induced PH: alveolar macrophage infiltration (AMI), AE, type II pneumocyte hyperplasia, and PE. In the groups treated with 50 and 100 mg/kg PRX-08066, the severity of lesions was significantly decreased compared with the MCT + VH rats (Fig. 6A). There was a significant reduction in AMI ($P < 0.05$) and AE ($P < 0.01$) in rats receiving MCT + 100 mg/kg PRX-08066 compared with the MCT + VH rats (Fig. 6B). The group that received MCT + 50 mg/kg PRX-08066 had significantly reduced AE ($P < 0.05$) compared only with the MCT + VH control. These results show a dose-dependent reduction of lung lesion characteristics with increasing doses of PRX-08066. The OLP is also markedly decreased with both treatment groups, but is significant only in the group treated with MCT + 100 mg/kg PRX-08066 versus the MCT + VH control ($P < 0.05$). Although the lung lesions in both drug groups were not completely prevented or cured, they were significantly diminished in both groups.

Reduction of Pulmonary Arterial Remodeling with PRX-08066. Medial wall thickness in the pulmonary arteries was markedly decreased in both treatment groups of PRX-08066 compared with the MCT + VH group as seen in the representative photomicrographs in Fig. 7A. The reduction of arterial thickness was observed not only in the tunica media, but also in the intima and adventitia regions. The decrease in overall arterial hypertrophy was significant between groups ($P < 0.002$) as determined by ANOVA (Fig. 7B). The arteriole wall thickness was increased, which resulted in the lumen-carrying capacity (L/TV%), shown in Fig. 7C, being markedly decreased in the MCT + VH group compared with the PBS + VH group (22.06 ± 1.92 and 54.09 ± 2.32, respectively; $P < 0.001$). Twice-daily dosing of both 50 and 100 mg/kg PRX-08066 attenuated an increase in pulmonary artery carrying capacity from that of the MCT + VH rats (36.72 ± 4.28 and 37.2 ± 2.88, respectively; $P < 0.01$).

Discussion

This study shows PRX-08066 attenuates the pathological effects of MCT-induced PAH in rats. MCT severely injures the pulmonary vasculature, ultimately resulting in increased vascular resistance and PAP, leading to RV pressure overload and RV hypertrophy similar to PAH seen in humans (Hessel et al., 2006). We demonstrated that the 5-HT2BR antagonist PRX-08066 prevented severe PAH and preserved cardiac function similar to control rats. Increased ejection fractions and decreased RV hypertrophy were observed by both MRI and pathologic analysis. Rats given PRX-08066

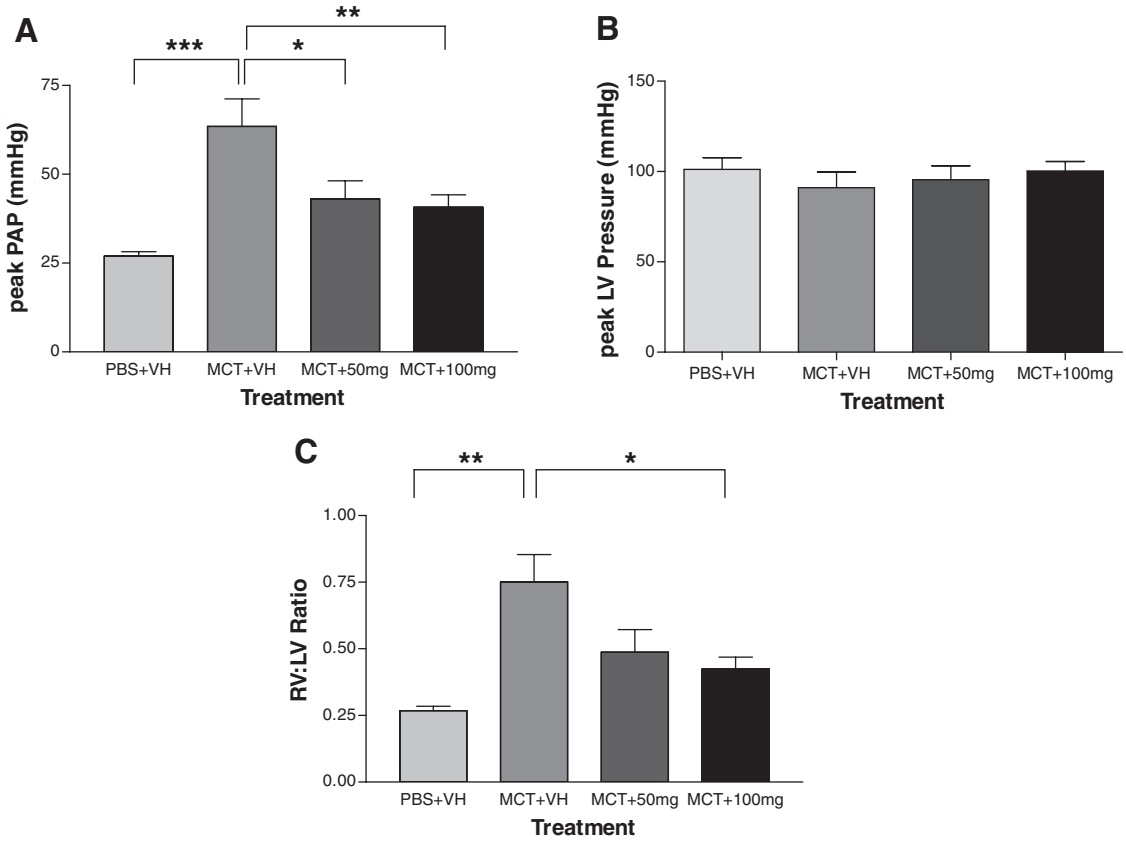

Fig. 4. The effects of PRX-08066 on hemodynamic function in the rat MCT model. A, there was a significant decrease in peak PAP in both PRX-08066 dosing groups compared with the rats that received MCT + VH (*, $P < 0.05$; **, $P < 0.01$; ***, $P < 0.001$). B, there was no difference seen in the peak LV pressure in any of the experimental groups. C, the 100 mg/kg dose of PRX-08066 demonstrated the greatest improvement for peak RV/LV ratio (*, $P < 0.01$; **, $P < 0.001$). Data are shown as the mean ± S.E.M.

TABLE 1

Body weight (BW), RV, and LV remodeling in rats treated with vehicle or PRX-08066 (50 or 100 mg/kg) on day 35 after administration of PBS or MCT

Values are means ± S.E.M.

	PBS + VH	MCT + VH	MCT + 50 mg PRX-08066	MCT + 100 mg PRX-08066
Body weight (kg)	0.336 ± 0.005*	0.269 ± 0.009	0.320 ± 0.007‡	0.294 ± 0.01†
RV/BW (g/kg)	0.61 ± 0.01*	1.31 ± 0.08	0.90 ± 0.10‡	0.87 ± 0.07*†
LV + S/BW (g/kg)	2.32 ± 0.07	2.16 ± 0.05	2.24 ± 0.04	2.20 ± 0.02
RV/ LV + S (g)	0.264 ± 0.01*	0.61 ± 0.04	0.40 ± 0.05‡	0.39 ± 0.03*†

* $P < 0.001$ vs. MCT-VH group.
† $P < 0.05$ vs. PBS-VH group.
‡ $P < 0.01$ vs MCT-VH group.

had improved lung pathology and reduced medial wall thickness consistent with prevention of severe MCT-induced PAH. We did not see a complete prevention of PAH, but treatment with PRX-08066, especially in rats receiving 100 mg/kg, resulted in a significant decrease in PAP and attenuated PAH development. The present results also did not prove a dose response between the 50 and 100 mg/kg doses of PRX-08066, which was confirmed by post-hoc Tukey multiple comparison analysis. However, both doses were effective in the majority of outcome measures, with a more optimal effect achieved at the 100 mg/kg dose. The lower p value in the 50 mg/kg treatment group was probably caused by lower animal numbers ($n = 8$) compared with the 100 mg/kg group ($n = 13$), which resulted in reduced statistical power. In addition, the study was not designed as a dose response study. The pathologic changes induced by MCT were not completely prevented, but were reduced in both dose groups.

This study also demonstrated tolerance of orally administered PRX-08066 twice a day without notable gastrointestinal side effects. Plasma levels of PRX-08066 in both dose groups showed linear pharmacokinetic behavior and good bioavailability through the oral route. PRX-08066 also attenuated the hemodynamic and pathologic characteristics of PAH. As part of the study protocol, rat weight changes were closely monitored. The group receiving 50 mg/kg PRX-08066 maintained close to normal rat weights compared with control. Although the group receiving 100 mg/kg gained less weight than the lower-dose group, they thrived compared with the MCT group. Despite the lower body weights of the group treated with 100 mg PRX-08066, the treatment resulted in a milder disease state with conserved cardiac function.

The chronic hypoxic mouse and MCT-induced rat models of PAH are used to evaluate the development, pathogenesis,

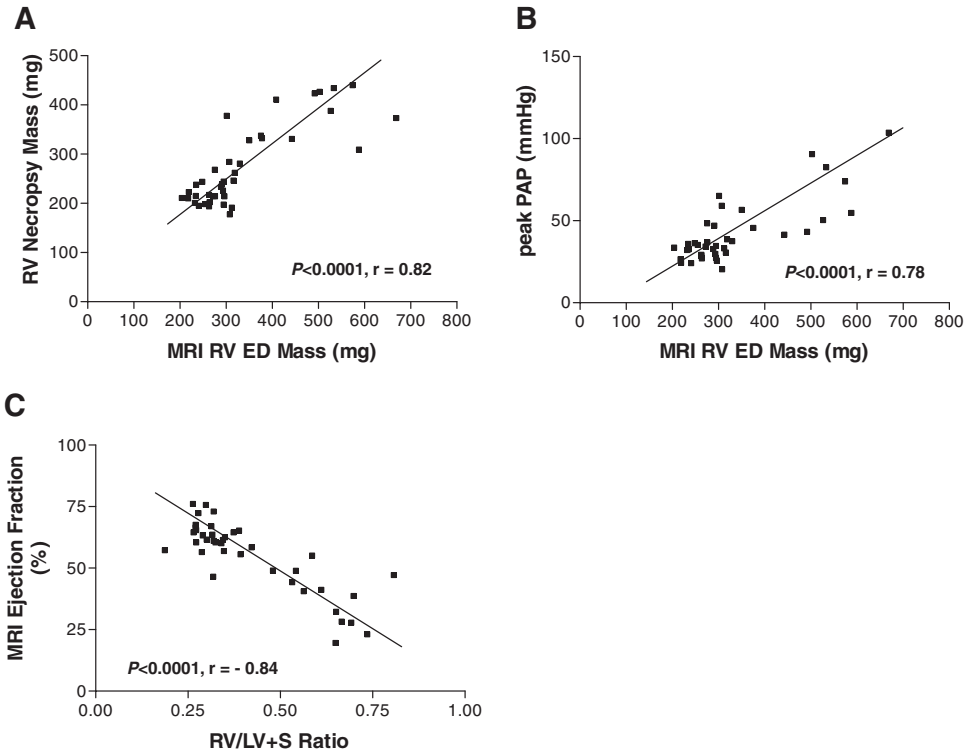

Fig. 5. Interaction of MRI cardiac function with hemodynamics and RV hypertrophy. A and B, positive linear correlations were observed between the RV mass at necropsy, peak PAP, and the MRI derived end-diastolic (ED) RV mass. C, a negative correlation was observed between MRI calculated ejection fraction and the weight ratio RV/LV+S.

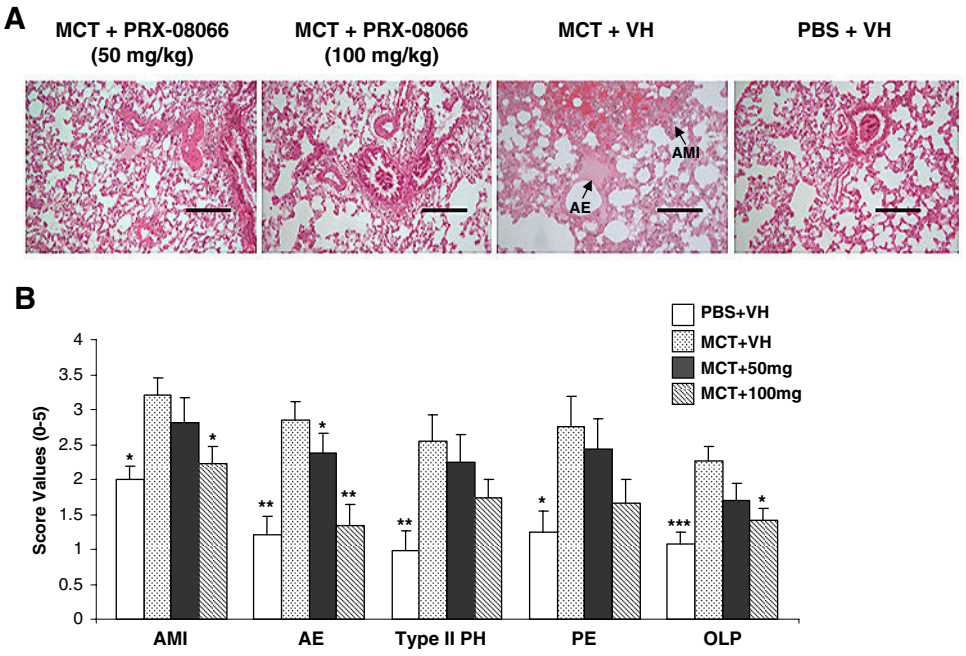

Fig. 6. Pathological evaluation of H&E lung tissue after treatment of PRX-08066. A, the 50 and 100 mg/kg doses of PRX-08066 both showed improvement in AMI and edema (AE), type II pneumocyte hyperplasia, and PE when evaluated against the MCT + VH control. Bars, 200 μm. B, the MCT + 100 mg/kg PRX-08066 group had significant reductions seen in the AMI (*, $P < 0.05$), AE (**, $P < 0.01$), and OLP (*, $P < 0.05$), whereas the MCT + 50 mg/kg PRX-08066 group showed marked improvement in AE (*, $P < 0.05$). PBS + VH versus MCT + VH (*, $P < 0.05$; **, $P < 0.01$; ***, $P < 0.001$). Data are shown as the mean ± S.E.M.

and treatment of PAH. Prior studies have investigated the role of 5-HT2BRs in the development of lung vascular remodeling and PAH by using the chronic hypoxic mouse model. Similar to our results, the 5-HT2BR antagonist, RS-127445 [4-(4-fluoro-1-naphthyl)-6-isopropylpyrimidin-2-amine], also demonstrated attenuation of PAH and prevented an increase in RV systolic pressure, RV/LV+S, and medial wall thickness in the chronic hypoxic mouse model (Launay et al., 2002; Callebert et al., 2006). These results differ from other findings that showed RS-127445 did not attenuate the development of MCT-induced PAH (Guignabert et al., 2005). That study used a dose of 2 mg/kg/day in the rat MCT model, and the lack of response may have resulted from the dose being too low.

Many PAH studies have targeted the main three pathways (prostacyclin, nitric oxide, and endothelin) for treatment using the MCT animal model. Our data demonstrate that PRX-08066 ameliorates the pulmonary vascular pathology similar to bosentan, sildenafil, beraprost, iloprost, and combinations of these drugs. PRX-08066 decreased PAP by 32% in the 50 mg/kg group and 36% in the 100 mg/kg group. A study using bosentan and sildenafil individually resulted in a 21% de-

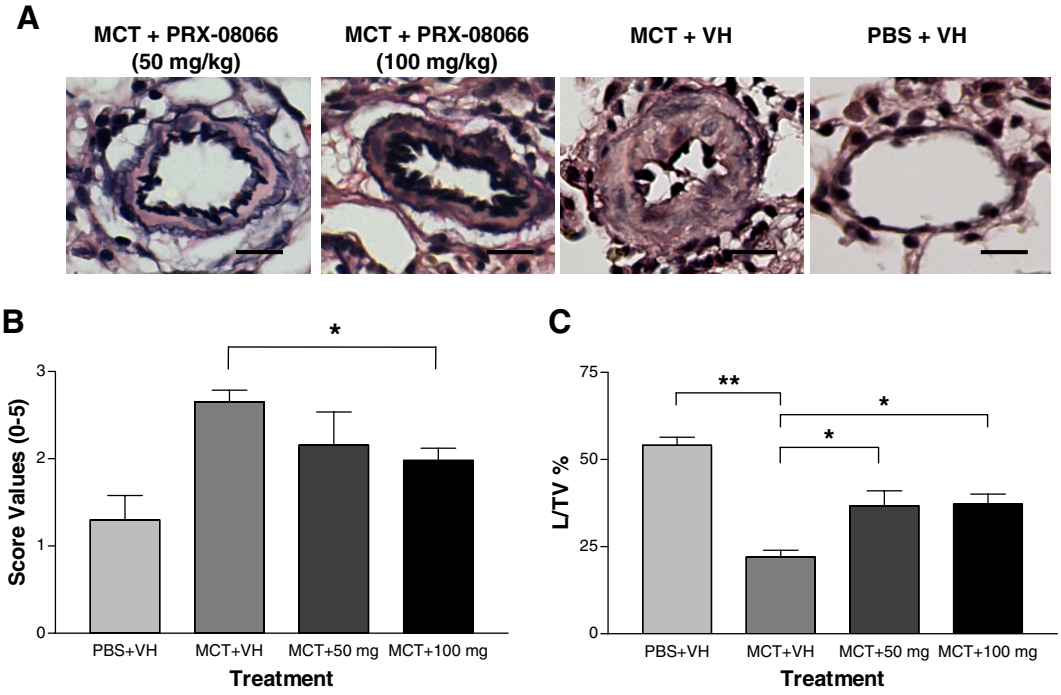

Fig. 7. Pulmonary artery remodeling after 5 weeks of PXR-08066 treatment. A, sections of lung tissue with the tunica intima, media, and adventitia are shown by Verhoeff-van Gieson staining for elastic lamina. Bars, 25 μm. B, the overall pathology of the pulmonary arteries was better in the PRX-08066 dose groups with the arterial wall thickness being reduced (ANOVA; $P < 0.002$). C, the ratio of lumen area to total vessel area (L/TV%) with treatment of PRX-08066 significantly prevented medial wall thickening and luminal occlusion compared with the MCT + VH group (*, $P < 0.01$; **, $P < 0.001$). Data are shown as the mean ± S.E.M.

crease, but the combination of the two drugs resulted in a 42% reduction in pressure (Clozel et al., 2006). Our study also showed less RV hypertrophy in the groups receiving 50 and 100 mg/kg PRX-08066 with a 34 and 36% decrease, respectively, which is comparable with the combination treatment of bosentan and sildenafil that resulted in a 37% reduction (Clozel et al., 2006). In a comparative study evaluating 2-{4-[(5,6-diphenylpyrazin-2-yl)(isopropyl)amino]butoxy}-*N*-(methylsulfonyl)acetamide (NS-304), a diphenylpyrazine derivative, with beraprost, the RV systolic pressure was decreased 25 and 17%, respectively and the reduction of RV hypertrophy was 24% for NS-304 and 12% for beraprost (Kuwano et al., 2008). Our results with PRX-08066 are also similar to the effect that inhaled and intravenous iloprost had on improving RV pressures (29 and 48%, respectively) and RV hypertrophy (35 and 40%, respectively) (Schermuly et al., 2004, 2005). Although PRX-08066 was not directly compared with bosentan, sildenafil, iloprost, or the other agents, our data revealed comparable or enhanced improvement as a monotherapy in the PAH pathology. Additional investigations looking at combinational therapies are important for improving long-term patient treatment and are already being reported (Schermuly et al., 2004; Kuwano et al., 2008).

Experimental studies evaluating therapies for PAH report results on improved RV function, PAP, and decreased pulmonary vasculature remodeling with little to no information on changes to LV function. The right and left ventricles are coupled, and with RV hypertension or volume overload there are changes in LV filling that impede cardiac output. As pulmonary vascular resistance (PVR) increases, it limits RV stroke volume. This decrease in volume output limits the volume available for LV filling (Marcus et al., 2001). As the LV filling decreases, there is less systemic cardiac output, and this was observed in the MCT-induced PAH rats that became systemically hypotensive. Contrary to previous reports with the 5HT2A receptor blocker ketanserin, which caused systemic hypotension (Frishman et al., 1995; Frishman and Grewall, 2000), our experiment demonstrated no significant change in the LV pressure between the treatment groups and the PBS controls, suggesting less peripheral vasodilatation with more selective vasodilatation of the pulmonary vasculature.

Cardiac MRI is a new noninvasive tool being used for the diagnosis, evaluation, and management of cardiac changes associated with PAH and the effects of therapeutic intervention on RV function and indices (van Wolferen et al., 2007; Chin et al., 2008). Changes in stroke volume, right and left ventricular volumes, and RV mass can be measured in response to therapeutic treatments. We have chosen this tool over echocardiography because of better consistency, lower operator variability, and more importantly, the fact that MRI can give functional data and reliable images of the RV morphology (Nagendran and Michelakis, 2007; Benza et al., 2008). The characteristic crescent-shaped RV was illustrated in the MR cardiac images from rats receiving PRX-08066 compared with MCT control rats. Both PRX-08066 treatment groups had a smaller RV mass and improved function with increased ejection fractions. MR images also showed that the PRX-08066 treatment regimen had no left ventricular septal bowing, which indicates a less severe increase in PVR. The structural changes demonstrated by MR evaluation correlated well with the decreased PAP seen in the PRX-08066 treatment groups. RV and LV hemodynamics are affected by geometric shape and wall thickness of the RV. The severity of pressure overload in the RV was decreased in the PRX-08066

treatment groups compared with the MCT control group, which developed a progressive afterload imposed by the PVR and resulted in left ventricular septal bowing and impaired LV filling.

Our results demonstrate that PRX-08066 attenuates the effect of MCT on the pulmonary vascular tree by decreasing the severity of PAH with decreased RV hypertrophy and PA pressure, reductions in histological changes and pulmonary arterial thickness, and improved RV function with increased ejection fractions. The 5-HT2BR antagonist can be targeted as an additional pathway toward the treatment of PAH. Further studies designed to demonstrate therapeutic rather than preventative effect need to be done to prove efficacy. This compound could prove effective as a single agent or in combination with other clinically available medications used in treatment of PAH.

Acknowledgments

We thank Barbara Locke, Lauren Schleenbaker, and the veterinary technicians for technical assistance; the animal care staff at the University of Florida; and the staff at the Advanced Magnetic Resonance Imaging and Spectroscopy facility at the University of Florida's McKnight Brain Institute.

References

Archer S and Rich S (2000) Primary pulmonary hypertension: a vascular biology and translational research "Work in progress." *Circulation* **102:**2781–2791.

Barst RJ, Rubin LJ, McGoon MD, Caldwell EJ, Long WA, and Levy PS (1994) Survival in primary pulmonary hypertension with long-term continuous intravenous prostacyclin. *Ann Intern Med* **121:**409–415.

Belohlávková S, Simák J, Kokesová A, Hnilicková O, and Hampl V (2001) Fenfluramine-induced pulmonary vasoconstriction: role of serotonin receptors and potassium channels. *J Appl Physiol* **91:**755–761.

Benza R, Biederman R, Murali S, and Gupta H (2008) Role of cardiac magnetic resonance imaging in the management of patients with pulmonary arterial hypertension. *J Am Coll Cardiol* **52:**1683–1692.

Callebert J, Esteve JM, Hervé P, Peoc'h K, Tournois C, Drouet L, Launay JM, and Maroteaux L (2006) Evidence for a control of plasma serotonin levels by 5-hydroxytryptamine (2B) receptors in mice. *J Pharmacol Exp Ther* **317:**724–731.

Chin KM, Kingman M, de Lemos JA, Warner JJ, Reimold S, Peshock R, and Torres F (2008) Changes in right ventricular structure and function assessed using cardiac magnetic resonance imaging in bosentan-treated patients with pulmonary arterial hypertension. *Am J Cardiol* **101:**1669–1672.

Clozel M, Hess P, Rey M, Iglarz M, Binkert C, and Qiu C (2006) Bosentan, sildenafil, and their combination in the monocrotaline model of pulmonary hypertension in rats. *Exp Biol Med (Maywood)* **231:**967–973.

D'Alonzo GE, Barst RJ, Ayres SM, Bergofsky EH, Brundage BH, Detre KM, Fishman AP, Goldring RM, Groves BM, and Kernis JT (1991) Survival in patients with primary pulmonary hypertension. Results from a national prospective registry. *Ann Intern Med* **115:**343–349.

Dempsie Y and MacLean MR (2008) Pulmonary hypertension: therapeutic targets within the serotonin system. *Br J Pharmacol* **155:**455–462.

Egermayer P, Town GI, and Peacock AJ (1999) Role of serotonin in the pathogenesis of acute and chronic pulmonary hypertension. *Thorax* **54:**161–168.

Esteve JM, Launay JM, Kellermann O, and Maroteaux L (2007) Functions of serotonin in hypoxic pulmonary vascular remodeling. *Cell Biochem Biophys* **47:**33–44.

Fitzgerald LW, Burn TC, Brown BS, Patterson JP, Corjay MH, Valentine PA, Sun JH, Link JR, Abbaszade I, Hollis JM, et al. (2000) Possible role of valvular serotonin 5-HT(2B) receptors in the cardiopathy associated with fenfluramine. *Mol Pharmacol* **57:**75–81.

Frishman WH and Grewall P (2000) Serotonin and the heart. *Ann Med* **32:**195–209.

Frishman WH, Huberfeld S, Okin S, Wang YH, Kumar A, and Shareef B (1995) Serotonin and serotonin antagonism in cardiovascular and noncardiovascular disease. *J Clin Pharmacol* **35:**541–572.

Guignabert C, Raffestin B, Benferhat R, Raoul W, Zadigue P, Rideau D, Hamon M, Adnot S, and Eddahibi S (2005) Serotonin transporter inhibition prevents and reverses monocrotaline-induced pulmonary hypertension in rats. *Circulation* **111:**2812–2819.

Hessel MH, Steendijk P, den Adel B, Schutte CI, and van der Laarse A (2006) Characterization of right ventricular function after monocrotaline-induced pulmonary hypertension in the intact rat. *Am J Physiol Heart Circ Physiol* **291:**H2424–H2430.

Hong Z, Olschewski A, Reeve HL, Nelson DP, Hong F, and Weir EK (2004) Nordexfenfluramine causes more severe pulmonary vasoconstriction than dexfenfluramine. *Am J Physiol Lung Cell Mol Physiol* **286:**L531–L538.

Kanai Y, Hori S, Tanaka T, Yasuoka M, Watanabe K, Aikawa N, and Hosoda Y (1993) Role of 5-hydroxytryptamine in the progression of monocrotaline induced pulmonary hypertension in rats. *Cardiovasc Res* **27:**1619–1623.

Kay JM, Smith P, and Heath D (1971) Aminorex and the pulmonary circulation. *Thorax* **26:**262–270.

Kew MC (1970) Aminorex fumarate: a double-blind trial and examination for signs of pulmonary arterial hypertension. *S Afr Med J* **44:**421–423.

Kramer MS and Lane DA (1998) Aminorex, dexfenfluramine, and primary pulmonary hypertension. *J Clin Epidemiol* **51:**361–364.

Kuwano K, Hashino A, Noda K, Kosugi K, and Kuwabara K (2008) A long-acting and highly selective prostacyclin receptor agonist prodrug, 2-{4-[(5,6-diphenylpyrazin-2-yl)(isopropyl)amino]butoxy}-*N*-(methylsulfonyl)acetamide (NS-304), ameliorates rat pulmonary hypertension with unique relaxant responses of its active form, {4-[(5,6-diphenylpyrazin-2-yl)(isopropyl)amino]butoxy}acetic acid (MRE-269), on rat pulmonary artery. *J Pharmacol Exp Ther* **326:**691–699.

Launay JM, Hervé P, Peoc'h K, Tournois C, Callebert J, Nebigil CG, Etienne N, Drouet L, Humbert M, Simonneau G, et al. (2002) Function of the serotonin 5-hydroxytryptamine 2B receptor in pulmonary hypertension. *Nat Med* **8:**1129–1135.

Li XQ, Hong Y, Wang Y, Zhang XH, and Wang HL (2006) Sertraline protects against monocrotaline-induced pulmonary hypertension in rats. *Clin Exp Pharmacol Physiol* **33:**1047–1051.

MacLean MR (1999) Pulmonary hypertension, anorexigens, and 5-HT: pharmacological synergism in action? *Trends Pharmacol Sci* **20:**490–495.

MacLean MR (2007) Pulmonary hypertension and the serotonin hypothesis: where are we now? *Int J Clin Pract Suppl* **156:**27–31.

MacLean MR, Herve P, Eddahibi S, and Adnot S (2000) 5-Hydroxytryptamine and the pulmonary circulation: receptors, transporters, and relevance to pulmonary arterial hypertension. *Br J Pharmacol* **131:**161–168.

Marcus JT, Vonk Noordegraaf A, Roeleveld RJ, Postmus PE, Heethaar RM, Van Rossum AC, and Boonstra A (2001) Impaired left ventricular filling due to right ventricular pressure overload in primary pulmonary hypertension: noninvasive monitoring using MRI. *Chest* **119:**1761–1765.

Miyata M, Ito M, Sasajima T, Ohira H, Sato Y, and Kasukawa R (2000) Development of monocrotaline-induced pulmonary hypertension is attenuated by a serotonin receptor antagonist. *Lung* **178:**63–73.

Nagendran J and Michelakis E (2007) MRI: one-stop shop for the comprehensive assessment of pulmonary arterial hypertension? *Chest* **132:**2–5.

Ohar JA, Waller KS, Williams TJ, Luke DA, and Demello DE (1998) Computerized morphometry of the pulmonary vasculature over a range of intravascular pressures. *Anat Rec* **252:**92–101.

Orbach M, Shacham S, Marantz M, Reddy S, Becker O, Maroteaux L, Ward W, Teoh H, Launay JM, Delacotte N, et al. (2006) PRX-08066: a potent 5-HT2B receptor antagonist with a dual mechanics for the treatment of pulmonary hypertension in *American Thoracic Society International Conference*; 2006 May 19–24; San Diego, CA. Abstract A420, American Thoracic Society, New York, NY.

Schermuly RT, Kreisselmeier KP, Ghofrani HA, Samidurai A, Pullamsetti S, Weissmann N, Schudt C, Ermert L, Seeger W, and Grimminger F (2004) Antiremodeling effects of iloprost and the dual-selective phosphodiesterase 3/4 inhibitor tolafentrine in chronic experimental pulmonary hypertension. *Circ Res* **94:**1101–1108.

Schermuly RT, Yilmaz H, Ghofrani HA, Woyda K, Pullamsetti S, Schulz A, Gessler T, Dumitrascu R, Weissmann N, Grimminger F, et al. (2005) Inhaled iloprost reverses vascular remodeling in chronic experimental pulmonary hypertension. *Am J Respir Crit Care Med* **172:**358–363.

van Wolferen SA, Marcus JT, Boonstra A, Marques KM, Bronzwaer JG, Spreeuwenberg MD, Postmus PE, and Vonk-Noordegraaf A (2007) Prognostic value of right ventricular mass, volume, and function in idiopathic pulmonary arterial hypertension. *Eur Heart J* **28:**1250–1257.

Yung D, Widlitz AC, Rosenzweig EB, Kerstein D, Maislin G, and Barst RJ (2004) Outcomes in children with idiopathic pulmonary arterial hypertension. *Circulation* **110:**660–665.

Zhou H, Liu H, Porvasnik SL, Terada N, Agarwal A, Cheng Y, and Visner GA (2006) Heme oxygenase-1 mediates the protective effects of rapamycin in monocrotaline-induced pulmonary hypertension. *Lab Invest* **86:**62–71.

Address correspondence to: Faris Al-Mousily, Department of Pediatrics, University of Florida, P.O. Box 100296, Gainesville, FL, 32610-0266. E-mail: al-mousily@pedcard.ufl.edu